ARTICLE

Spontaneous Curling of Graphene Sheets with Reconstructed Edges

Vivek B. Shenoy,[†,*] Chilla Damodara Reddy,[‡] and Yong-Wei Zhang[‡]

[†]School of Engineering, Brown University, Providence, Rhode Island 02912 and [‡]Institute of High Performance Computing, 1 Fusionopolis Way, #16-16 Connexis, Singapore 138632

ABSTRACT Recent microscopy experiments have revealed novel reconstructions of the commonly observed zigzag and armchair edges in graphene. We show that tensile edge stresses at these reconstructed edges lead to large-scale curling of graphene sheets into cylindrical surfaces, in contrast to the warping instabilities predicted for unreconstructed edges. Using atomic-scale simulations and large deformation plate models, we have derived scaling laws for the curvature and strain of the curled sheets in terms of the edge stress, shape, and the bending and stretching moduli. For graphene nanoribbons, we show that tensile edge stress leads to periodic ripples, whose morphologies are distinct from those observed due to thermal fluctuations or thermally generated mismatch strains. Since the electronic properties of graphene can be altered by both curvatures and strain, our work provides a route for potentially fabricating nanoelectronic devices such as sensors or switches that can detect stresses induced by dopants at the edges.

KEYWORDS: graphene · curling · edge reconstruction · edge stress · molecular dynamics simulations · finite element simulations

Graphene, a single sheet of carbon atoms, has attracted a lot of interest since it was isolated from bulk graphite a few years back.[1] The unique band structure of this 2D material and the near massless behavior of its charge carriers give rise to many interesting electronic and transport properties.[2] While graphene is gapless, a band gap can be opened by cutting graphene sheets into 1D nanoribbons or 0D quantum dots. The band gap of such nanostructures depends on both the edge type and ribbon widths or dot sizes, making graphene a very interesting material for potential electronics applications. Recent theoretical and experimental work has shown that the edges of graphene nanoribbons strongly influence their electronic and magnetic properties. Therefore, much effort has been devoted to controlling the structure of edges in graphene.[2]

While graphene is normally terminated by zigzag and armchair edges, recent theoretical calculations have predicted the existence of new reconstructed structures,[3] which have since been observed in high-resolution microscopy experiments (Figure 1).[4,5] Among all the possible edge structures, first-principle calculations show that the zigzag edges reconstructed with five- and seven-membered carbon rings are most favorable from an energetic point of view since they contain fewer dangling bonds at the edges.[3] More significantly, recent work also shows that reconstructions can alter the state of stresses at the edges.[6,7] While the edge stresses in zigzag and armchair edges are compressive,[6−8] atomistic calculations predict that both the 5−7 reconstructed edges[7] (Figure 1a) and 5−6 reconstructed armchair edges[6] (Figure 1b) are under states of tensile edge stresses. It has been shown that compressive stresses at zigzag and armchair edges lead to warping and twisting instabilities in graphene sheets and nanoribbons.[9,10] Warping and rippling of graphene nanostructures have also been observed recently.[11] Given the fact that low-energy reconstructed edges are under a state of tensile stress, a natural question to ask is whether instabilities are expected in this case, and if so, what the nature of these instabilities are, and how they differ from those of zigzag and armchair cases.

In this article, using a combination of atomistic simulations and continuum models for large deformations of elastic plates, we show that, in distinct contrast to unreconstructed edges, tensile stresses at the reconstructed edges lead to curling up of graphene sheets into cylindrical surfaces with tapered ends and to rippling of nanoribbons. The key difference that results in distinct morphologies for the two cases is the propensity of the edge to stretch (shrink) under the influence of compressive (tensile) edge stresses. While out-of-plane

*Address correspondence to vivek_shenoy@brown.edu.

Received for review April 21, 2010 and accepted July 20, 2010.

Published online July 27, 2010.
10.1021/nn100842k

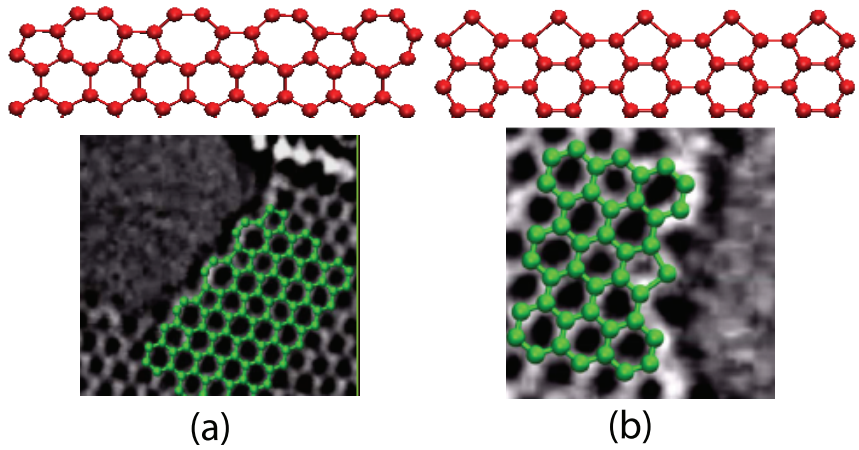

Figure 1. (Top) Graphene sheets with zigzag and armchair edges reconstructed with pentagon−heptagon (a) and pentagon−hexagon (b) structures, respectively. (Bottom) Reconstructed structures observed in recent experiments.[4,5]

warping from the initially flat configuration will always lead to stretching, for the edges to shrink, as we show below, the sheets have to first curl into a nearly cylindrical surface. The curvatures of the curled structures depend on the magnitude of the edge stresses, the dimensions of the sheets, and both the bending and stretching moduli of the sheets. In addition, we find that long and narrow nanoribbons can adopt rippled morphologies that consist of curved segments of nearly equal curvature and large strain at the edges. Using continuum plate models, we have derived closed-form analytical solutions for the curvatures and strains in curled sheets that are in excellent agreement with atomistic simulations. While we have confined our attention to cases where tensile stresses are induced by reconstructions, our theory also applies to cases where stresses arise due to adsorption of atoms on or in the vicinity of the edges. Since the electronic properties can be altered by both curvatures and strain,[2] our work provides a route for engineering the deformation of the sheets by partially or fully decorating the edges.

RESULTS AND DISCUSSION

Here, the instabilities of reconstructed edges are studied using the reactive bond order (AIREBO)[12] potential as implemented in the molecular dynamics package LAMMPS[13] (see Methods). First, we consider a nearly square-shaped sheet where the armchair and zigzag edges are reconstructed with 5−6 and 5−7 structures, respectively. For the former case, the AIREBO potential predicts an edge stress of 24.4 eV/nm while the stress in the latter case is only 0.02 eV/nm. Since the edge stress is negligible in the latter case, the instabilities that we study arise solely from the 5−6 structure. Upon relaxation, the sheets curl about an axis perpendicular to the armchair edge with their ends arching inward, as shown in Figure 2. We find two modes of curling; the first mode is a cylindrical surface with tapered ends, while the second mode is composed of two cylindrical surfaces with curvatures that are opposite in sign but are equal in magnitude to that of the first mode and are smoothly connected at the center of the sheet. Compared to the relaxed planar configuration, curling leads to an energy gain of 11.7 and 5.6 eV for the first and second modes, respectively.

To study the effect of geometry on curling, next we consider the shapes of nanoribbons whose long edges are terminated by 5−6 armchair edges with large tensile stresses (Figure 3). Here, we show three modes which are composed of segments of cylindrical surfaces with tapered ends and whose curvatures alternate in sign from one end of the ribbon to the other. The magnitudes of the curvatures of each of these segments are, however, nearly equal. In this regard, there are important differences between the "ripples" induced by tensile stresses seen in Figure 3b,c and those induced by compressive stresses arising from unreconstructed edges[9,10] as well as sinusoidal ripples seen in suspended nanoribbons due to thermal strains.[14] Unlike the ripples in Figure 3, ripples due to compressive stresses are localized at the edges. For the sinusoidal ripples in suspended films, the curvatures vary in a sinusoidal manner across the length of the ribbon, whereas the ripples in Figure 3 are characterized by segments of nearly constant curvature. We also note that as in the case of the curled shapes of sheets in Figure 2, from an energetic point of view, modes with fewer "domain" boundaries, where the curvatures switch sign, are lower in energy; the energy gained by formation of mode (a) in Figure 3 is higher than that of (b) and (c) by 2.2 and 10.3 eV, respectively.

Why do the sheets curl and how are the curvatures related to the edge stresses and the elastic properties of the sheet? We answer these questions next using both finite element simulations and a large deformation model for elastic plates. In our finite element model, graphene is modeled as an elastic plate, whose Young's modulus E_p and thickness t are computed by equating the effective 2D modulus, $E_p t = E = 2000$ eV/nm^2,[9,15] and flexural rigidity to the bending modu-

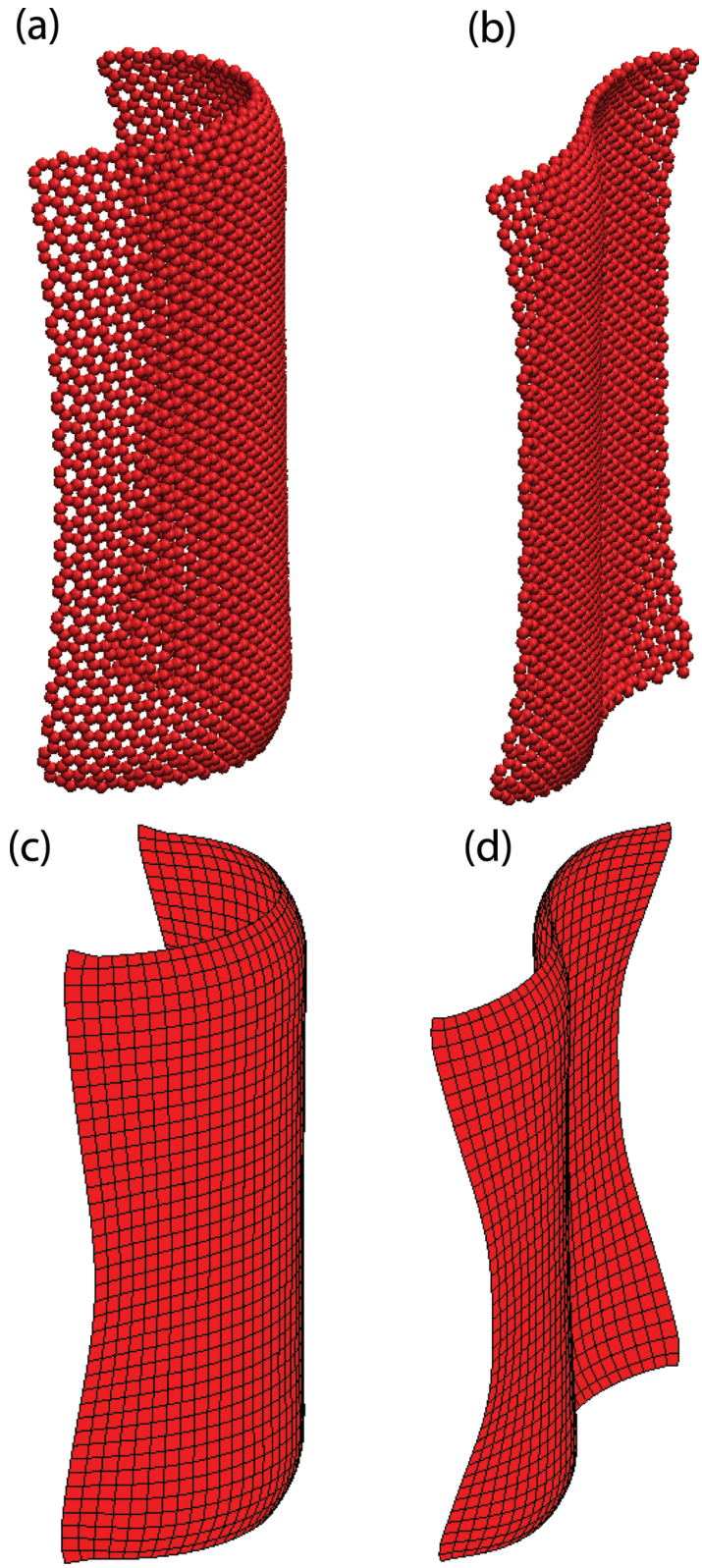

Figure 2. (a,b) Shapes of curled 8.24 nm (armchair) × 8.23 nm (zigzag) edge-reconstructed graphene sheets obtained by relaxing perturbed graphene lattice with the AIREBO potential. (c,d) Curled shapes obtained from finite element simulations that explicitly account for tensile edge stresses.

lus of graphene, $E_p t^3/12(1-\nu^2) = M_b = 1$ eV. Residual stresses corresponding to the edge stresses for reconstructed armchair and zigzag orientations are assigned to the finite elements at the appropriate edges of the sheet. The results of our simulations are given in Figures 2 and 3. In all cases, the deformed sheets closely resemble the shapes observed in atomistic simulations, confirming that tensile edge stresses are responsible for the curling of the sheets.

Next, we develop an analytical description of curling using the Föppl-von-Kármán[16] (FvK) large deflection theory for elastic plates. Our goal is to determine how the radius of curvature (R_0), the edge deflection (A_r), and the penetration depth (λ_r) depend on the material and geometric parameters (refer to Figure 4). To this end, we consider the kinematics of curling which involves (1) pure bending of the flat sheet to a cylindrical surface without any stretching and (2) displacement of the material points on this cylinder initially at (R_0, z), both radially and along the cylinder axis, so that the new coordinates (R, Z) can be written as

$$R = R_0 + u_r(z),\ Z = z + u_z(z) \tag{1}$$

where u_i are the displacement fields. On the basis of FvK theory, the principal strains and curvatures arising from this deformation field are

$$\varepsilon_a = u_z' + \frac{1}{2}u_r'^2,\ \varepsilon_\theta = \frac{u_r}{R_0}$$
$$\kappa_a = \frac{-u_r''}{(1+u_r'^2)^{3/2}},\ \kappa_\theta = \frac{1}{R(1+u_r'^2)^{1/2}} \tag{2}$$

where $'$ indicates differentiation with respect to z, and a and θ denote, respectively, the axial and circumferential components. Using these fields, the edge, stretching, and bending energies per unit length of the 5−6 armchair edge can be written as

$$E_e = 2\tau\varepsilon_\theta\Big|_{z=0}$$
$$E_s = M\int_0^{L/2}(\varepsilon_a^2 + \varepsilon_\theta^2 + 2\nu\varepsilon_a\varepsilon_\theta)dz \tag{3}$$
$$E_b = M_b\int_0^{L/2}(\kappa_a^2 + \kappa_\theta^2 + 2\nu\kappa_a\kappa_\theta)dz$$

where τ is the edge stress, $M = E/(1-\nu^2)$ is the stretching modulus in which E and ν are the 2D Young's modulus and Poisson's ratio, respectively, and M_b is the bending modulus. Note that each of the terms in eq 3 has been multiplied by 2 to account for the contributions from the top and bottom halves.

A variational solution to the FvK equations can be obtained by using the ansatz

$$u_r = -A_r e^{-z/\lambda_r},\ u_z = A_z e^{-z/\lambda_z} \tag{4}$$

where A_i and λ_i are, respectively, the amplitudes and penetration depths of the displacement fields. These parameters and the radius R_0 can then be determined by minimizing the total energy, $E_t = E_e + E_s + E_b$. While this can be readily carried out numerically, we have found that accurate and compact closed-form expres-

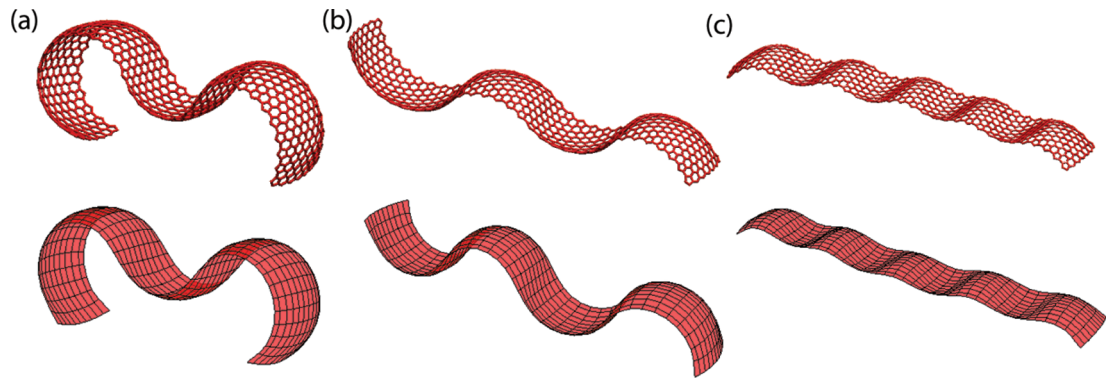

Figure 3. (Top) Shapes of warped 13.2 nm (armchair) × 1.7 nm (zigzag) edge-reconstructed graphene nanoribbons obtained by relaxing perturbed graphene lattices with the AIREBO potential. (Bottom) Shapes of graphene nanoribbons obtained from finite element simulations that explicitly account for tensile edge stresses.

sions can be found if terms proportional to the Poisson's ratio in eq 3 are ignored. As we show below, for graphene with $\nu \approx 0.15$,[17] retaining these terms leads to very small (<5%) differences in the variational parameters. If these terms are ignored, the total energy is quadratic in the circumferential strain, and this contribution vanishes when $A_z = 1/4(A_r^2/\lambda_r)$ and $\lambda_z = \lambda_r/2$. Using this result in eq 3, the total energy can be expressed as

$$E_t = -2\tau\frac{A_r}{R_0} + \frac{1}{2}M\frac{A_r^2\lambda_r}{R_0^2} + \frac{1}{2}M_b\frac{L}{R_0^2} + \frac{1}{2}M_b\frac{A_r^2}{\lambda_r^3} \quad (5)$$

Minimizing the total energy, we obtain the parameters that characterize the deformation of curled sheets and the compressive strain $\varepsilon_0 = A_r/R_0$ at the edge:

$$\begin{aligned} R_0 &= \frac{2^{4/3}L^{2/3}M^{1/2}M_b^{5/6}}{3^{1/2}\tau^{4/3}} \\ A_r &= \frac{3^{1/2}}{2^{1/3}}\frac{L^{1/3}M_b^{1/6}\tau^{1/3}}{M^{1/2}} \\ \lambda_r &= 2^{2/3}\frac{L^{1/3}M_b^{2/3}}{\tau^{2/3}} \\ \varepsilon_0 &= \frac{3}{2^{5/3}}\frac{\tau^{5/3}}{L^{1/3}MM_b^{2/3}} \end{aligned} \quad (6)$$

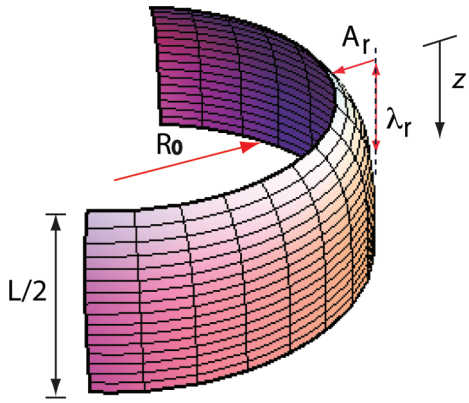

Figure 4. Schematic of the top-half of curled graphene sheets. The symbols are explained in the text.

It is interesting to note that the maximum strain and curvature increase with decreasing width, L. This is clearly seen in Figure 3, where the nanoribbons are much more curved compared to the wider sheet considered in Figure 2.

A comparison of the predictions of the analytical model with atomistic simulations and numerical minimization of the total energy in eq 3 (where we retain the terms proportional to the Poisson's ratio) is given in Table 1. We find very good agreement of the analytical results with both atomistic simulations and numerical results. It is interesting to note that the strain at the edge and radius of curvature in the case of nanoribbons in Figure 3 with a width of 1.7 nm can be as large as ~14% and 1.3 nm, respectively. Since both strain and curvature scale inversely with the width and the electronic properties strongly depend on state of deformation, the electronic structure of the curled and rippled structures can be considerably different from that of planar nanoribbons. First-principle calculations predict an edge stress of 12 eV/nm for the 5−7 zigzag reconstruction;[7] the deformation in this case can be analyzed following the continuum models developed here.

While this article was under review, a report[18] appeared of the observation of spontaneous curving of graphene flakes due to formation of pentagon rings at the edges similar to the cases considered in our work. Transmission electron microscopy studies show that curving eventually leads to formation of fullerenes. The four critical steps in a top-down mechanism of fullerene

TABLE 1. Radius of Curvature (R_0), Edge Deflection (A_r), and Penetration Depth (λ_r) Obtained Using Different Approaches[a]

	AIREBO			analytical			numerical		
size	R_0	A_r	λ_r	R_0	A_r	λ_r	R_0	A_r	λ_r
8.24 × 8.23	3.75	0.18	0.38	3.89	0.19	0.39	3.87	0.18	0.39
16.62 × 16.45	6.00	0.31	0.61	6.01	0.23	0.48	6.14	0.23	0.49
13.2 × 1.7	1.28	0.19	0.35	1.31	0.11	0.22	1.39	0.11	0.24

[a] All lengths are given in nanometers. For the analytical and numerical calculations, we have used $\tau = 24.4$ eV/nm, $M = 2000$ eV/nm^2, and $M_b = 1$ eV.

formation are (i) loss of carbon atoms at the edge of graphene, leading to (ii) the formation of pentagons, which (iii) triggers the curving of graphene into a bowl-shaped structure and which (iv) subsequently zips up its open edges to form a closed fullerene structure. These structures are formed in both free-standing flakes and on flakes resting on graphene sheets, indicating that the driving force for curling is able to overcome the interactions with the underlying support.

CONCLUSIONS

In summary, we have shown that tensile stresses at the reconstructed graphene edges lead to instabilities that are distinct from the instabilities in zigzag- and armchair-terminated sheets and nanoribbons. In particular, these stresses lead to curling of graphene sheets and nanoribbons as well as significant strain at the edges. Compared to the case of compressive edge stress, the deformation/curvature we have observed here can span the entire size of the sample. We have derived analytical results that give the scaling of the curvature as a function of edge stress and other material and geometric parameters. Since edge stresses can be engineered by functionalizing the edges or by doping regions close to the edge, our analytical results can be used to study instabilities in these cases. Deformation of graphene sheets arising from curvature and spatially varying strain fields can lead to novel devices and phenomena including valley filtering and creation of effective magnetic fields leading to zero-field quantum Hall effect;[19] therefore, there is great interest in methods for creating rippled and folded/curved graphene sheets in a controlled manner.[14] Our work provides clear guidelines for engineering the deformation by controlling edge stresses. Finally, as the shape of the deformed sheets depends strongly on the stresses induced by dopants at the edges, graphene sheets could potentially find applications as a switch or a sensor.

METHODS

The instabilities of reconstructed edges are studied using the reactive bond order (AIREBO)[12] potential as implemented in the molecular dynamics package LAMMPS.[13] This potential allows for covalent bond breaking and creation with associated changes in atomic hybridization within a classical potential, thus enabling simulations of nano- and micrometer-size sheets. In order to study the stability of flat free-standing sheets, we first perturb them by allowing random out-of-plane displacement to the atoms. The atoms in the perturbed sheet are then allowed to relax using a conjugate gradient algorithm implemented in LAMMPS[13] with an energy tolerance of 10^{-10} eV. The finite element simulations were carried out using the Abaqus package (Simulia Inc., Providence, RI). We treat graphene as an elastic plate with bending and stretching moduli determined as explained in the main text. Residual strain at the edges is applied by calibrating the thermal expansion coefficients at the edge elements to obtain appropriate edge stresses. As in the atomistic simulations, we apply an initial perturbation to a nominally flat sheet and allow it to relax. All simulations are carried out in a finite deformation setting; that is, the effect of geometry changes on force balance and rigid body rotations are explicitly taken into account.

Acknowledgment. The research support of the NSF and NRI through the Brown University MRSEC and the NSF through Grants CMMI-0825771, DMS-0854919, and DMS-0914648 is gratefully acknowledged. Computational support for this research was provided by Grant TG-DMR090098 from the TeraGrid advanced support program and the Center for Computation and Visualization at Brown University.

REFERENCES AND NOTES

1. Novoselov, K. S.; Geim, A. K.; Morozov, S. V.; Jiang, D.; Zhang, Y.; Dubonos, S. V.; Grigorieva, I. V.; Firsov, A. A. Electric field effect in atomically thin carbon films. *Science* **2004**, *306*, 666–669.
2. Castro Neto, A. H.; Guinea, F.; Peres, N. M. R.; Novoselov, K. S.; Geim, A. K. The electronic properties of graphene. *Rev. Mod. Phys.* **2009**, *81*, 109–162.
3. Koskinen, P.; Malola, S.; Hakkinen, H. Self-passivating edge reconstructions of graphene. *Phys. Rev. Lett.* **2008**, *101*, 115502.
4. Girit, C. O.; Meyer, J. C.; Erni, R.; Rossell, M. D.; Kisielowski, C.; Yang, L.; Park, C. H.; Crommie, M. F.; Cohen, M. L.; Louie, S. G. Graphene at the edge: stability and dynamics. *Science* **2009**, *323*, 1705–1708.
5. Koskinen, P.; Malola, S.; Hakkinen, H. Evidence for graphene edges beyond zigzag and armchair. *Phys. Rev. B* **2009**, *80*, 073401.
6. Reddy, C. D.; Ramasubramaniam, A.; Shenoy, V. B.; Zhang, Y. W. Edge elastic properties of defect-free single-layer graphene sheets. *Appl. Phys. Lett.* **2009**, *94*, 101904.
7. Huang, B.; Liu, M.; Su, N. H.; Wu, J.; Duan, W. H.; Gu, B. L.; Liu, F. Quantum manifestations of graphene edge stress and edge instability: a first-principles study. *Phys. Rev. Lett.* **2009**, *102*, 166404.
8. Jun, S. Density-functional study of edge stress in graphene. *Phys. Rev. B* **2008**, *78*, 073405.
9. Shenoy, V. B.; Reddy, C. D.; Ramasubramaniam, A.; Zhang, Y. W. Edge-stress-induced warping of graphene sheets and nanoribbons. *Phys. Rev. Lett.* **2008**, *101*, 245501.
10. Bets, K. V.; Yakobson, B. I. Spontaneous twist and intrinsic instabilities of pristine graphene nanoribbons. *Nano Res.* **2009**, *2*, 161–166.
11. Li, Z. J.; Cheng, Z. G.; Wang, R.; Li, Q.; Fang, Y. Spontaneous formation of nanostructures in graphene. *Nano Lett.* **2009**, *9*, 3599–3602.
12. Stuart, S. J.; Tutein, A. B.; Harrison, J. A. A reactive potential for hydrocarbons with intermolecular interactions. *J. Chem. Phys.* **2000**, *112*, 6472–6486.
13. Plimpton, S. Fast parallel algorithms for short-range molecular-dynamics. *J. Comput. Phys.* **1995**, *117*, 1–19.
14. Bao, W. Z.; Miao, F.; Chen, Z.; Zhang, H.; Jang, W. Y.; Dames, C.; Lau, C. N. Controlled ripple texturing of suspended graphene and ultrathin graphite membranes. *Nat. Nanotechnol.* **2009**, *4*, 562–566.
15. Lee, C.; Wei, X. D.; Kysar, J. W.; Hone, J. Measurement of the elastic properties and intrinsic strength of monolayer graphene. *Science* **2008**, *321*, 385–388.
16. Landau, L. D.; Lifshitz, E. M. *Theory of Elasticity*, 3rd ed.; Oxford: New York, 1986.
17. Kudin, K. N.; Scuseria, G. E.; Yakobson, B. I. C2F, BN, and C nanoshell elasticity from *ab initio* computations. *Phys. Rev. B* **2001**, *64*, 10.
18. Chuvilin, A.; Kaiser, U.; Bichoutskaia, E.; Besley, N. A.; Khlobystov, A. N. Direct transformation of graphene to fullerene. *Nat. Chem.* **2010**, *2*, 450–453.
19. Guinea, F.; Katsnelson, M. I.; Geim, A. K. Energy gaps and a zero-field quantum Hall effect in graphene by strain engineering. *Nat. Phys.* **2010**, *6*, 30–33.